Tumor Characterization by Ultrasound Elastography and Contrast-Enhanced Ultrasound

19

Thomas Fischer, Anke Thomas, and Dirk-André Clevert

Abstract

State-of-the-art techniques of ultrasound elastography can contribute to the characterization of focal breast lesions and detection of malignant tumors in various organs. Another area of current interest is the differentiation of focal liver lesions in terms of vascularization patterns measured by perfusion ultrasound. This chapter provides an overview of the different techniques and their diagnostic role in clinical routine based on a review of the current literature. The most important techniques are compression or vibration elastography, shear wave elastography (SWE), and contrast-enhanced ultrasound (CEUS). Currently available scientific evidence suggests that elastography provides important supplementary information for the differentiation of breast lesions under routine clinical conditions. The information is immediately available and improves specificity. Strain ratio (SR) is especially useful in women with a high pretest likelihood of breast cancer. Prostate cancer also shows characteristic differences in terms of elastographic properties compared with surrounding tissue. Here, elastography can improve targeted biopsy for the workup of suspicious focal lesions and is superior to routine prostate biopsy guided by B-mode ultrasound. CEUS has high diagnostic accuracy and is comparable to computed tomography (CT) and magnetic resonance imaging (MRI) in terms of tumor characterization. Having a low rate of

T. Fischer (✉)
Department of Radiology, Institut für Radiologie und Ultraschallforschungslabor, Charité – Universitätsmedizin Berlin, Berlin, Germany
e-mail: thom.fischer@charite.de

A. Thomas
Ultraschallforschungslabor, Charité – Universitätsmedizin Berlin, Berlin, Germany

D.-A. Clevert
Institut für Klinische Radiologie, Klinikum der Universität München-Grosshadern, München, Germany

I. Sack, T. Schaeffter (eds.), *Quantification of Biophysical Parameters in Medical Imaging*, https://doi.org/10.1007/978-3-319-65924-4_19

adverse effects, CEUS can be used in patients with impaired renal function or contraindications to CT or MRI contrast agents. Quantifiable elastography and CEUS have recently started to expand the role of classic B-mode ultrasound in oncology. Quantification of tumor stiffness and perfusion can improve the differential diagnosis. These two ultrasound techniques are beginning to enter the clinic and offer a fascinating potential for further advances including improved standardization of ultrasound diagnosis.

19.1 Part A: Application of Ultrasound Elastography

19.1.1 Introduction

Tissues have inherent elasticity, which changes with normal aging or when disease such as inflammation or a tumor is present. A variety of ultrasound techniques, jointly known as sonoelastography, have been developed since the early 1990s to assess the elasticity of biological tissues [1–3] (see Chap. 12). The external force required to induce tissue deformation depends on the tissue's shear modulus [4, 5] and appears to be altered in tumor tissue (see Chaps. 2 and 5 for constitutive equations and biophysical background). Clinical studies in different organ systems have shown that determination of tissue elasticity provides important supplementary diagnostic information. The organs investigated include the parotid [6], thyroid [7, 8], liver [9, 10], prostate [11], and cervix [12]. Special attention has been paid to the sonoelastographic characterization of tumorous lesions in the breast [13–15] and prostate. For breast imaging, it has been shown that using tissue elasticity as an additional criterion improves specificity [13–17] and lowers the number of false-positive findings [14]. Breast sonoelastography thus has the potential to reduce the need for biopsy in the future. An important clinical advantage of sonoelastography is that it is generally available and quick to perform at little extra cost. The high spatial resolution of ultrasound allows determination of the elastic properties of small structures (less than 5 mm). On the other hand, sonoelastography has some technical disadvantages including the limited penetration depth of only 5–6 cm (for transient-based techniques), sensitivity to the axial displacement component only, and the examiner dependence. More details on the comparison between state-of-the art sonoelastographic modalities can be found in Chap. 12. The following sections present clinical applications of sonoelastography in the diagnostic evaluation of malignant tumors of the breast, thyroid, and prostate.

19.1.2 Breast Cancer

Breast lesions may be very small (on the order of 5 mm), and their detection therefore requires an elastographic imaging technique with high spatial resolution. Research has focused on techniques using absence of elasticity for the evaluation of focal breast lesions. This criterion contributes to the characterization of breast

lesions detected by ultrasound. The use of tissue elasticity as an additional diagnostic parameter has been shown to increase specificity and to improve the separation of benign and malignant focal lesions classified as BI-RADS (Breast Imaging Reporting and Data System) category 3 or 4 [18]. The technique thus reduces the number of false-positive findings and could spare many women unnecessary breast biopsies in the future. When the technique was first introduced, differentiation of benign and malignant breast lesions relied on subjective and/or semi-quantitative approaches (Fig. 19.1a, b).

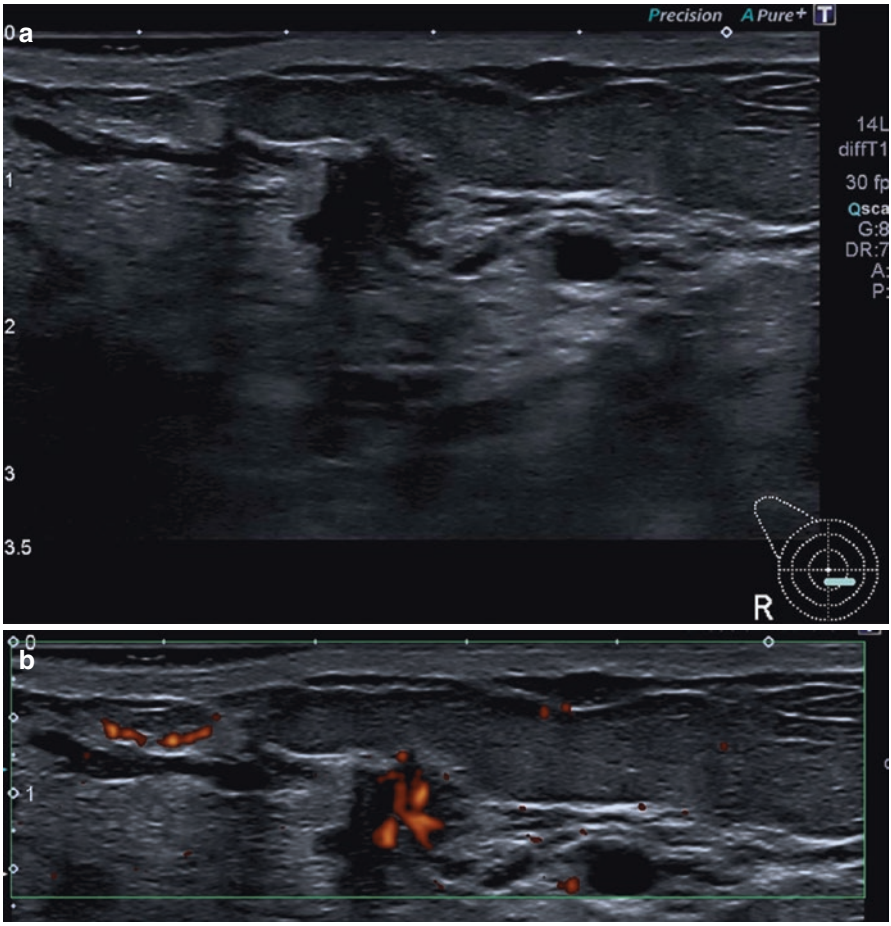

Fig. 19.1 A 48-year-old patient presenting with a suspicious lesion palpated in the right breast. The ultrasound B-mode image shows an irregular, microlobulated, spiculated focal lesion measuring 1.2 cm with marked ductal dilation in the vicinity of the lesion (**a**). The B-mode appearance is consistent with a BI-RADS 5 lesion. Ductal dilation in the vicinity of the lesion may indicate a DCIS component. There is ample perfusion of the lesion and a vessel entering the focal lesion perpendicularly (**b**). TDI shows complete absence of color pixels in the lesion, consistent with incompressibility (**c**). Both techniques confirm breast cancer. The fat-to-lesion strain ratio (FLR) is only slightly elevated at 1.62 (**d**). Shear wave elastography (SWE) shows faster transmission of signals through the breast lesion (**e**), which is reflected in an increase in the SWE ratio (**f**)

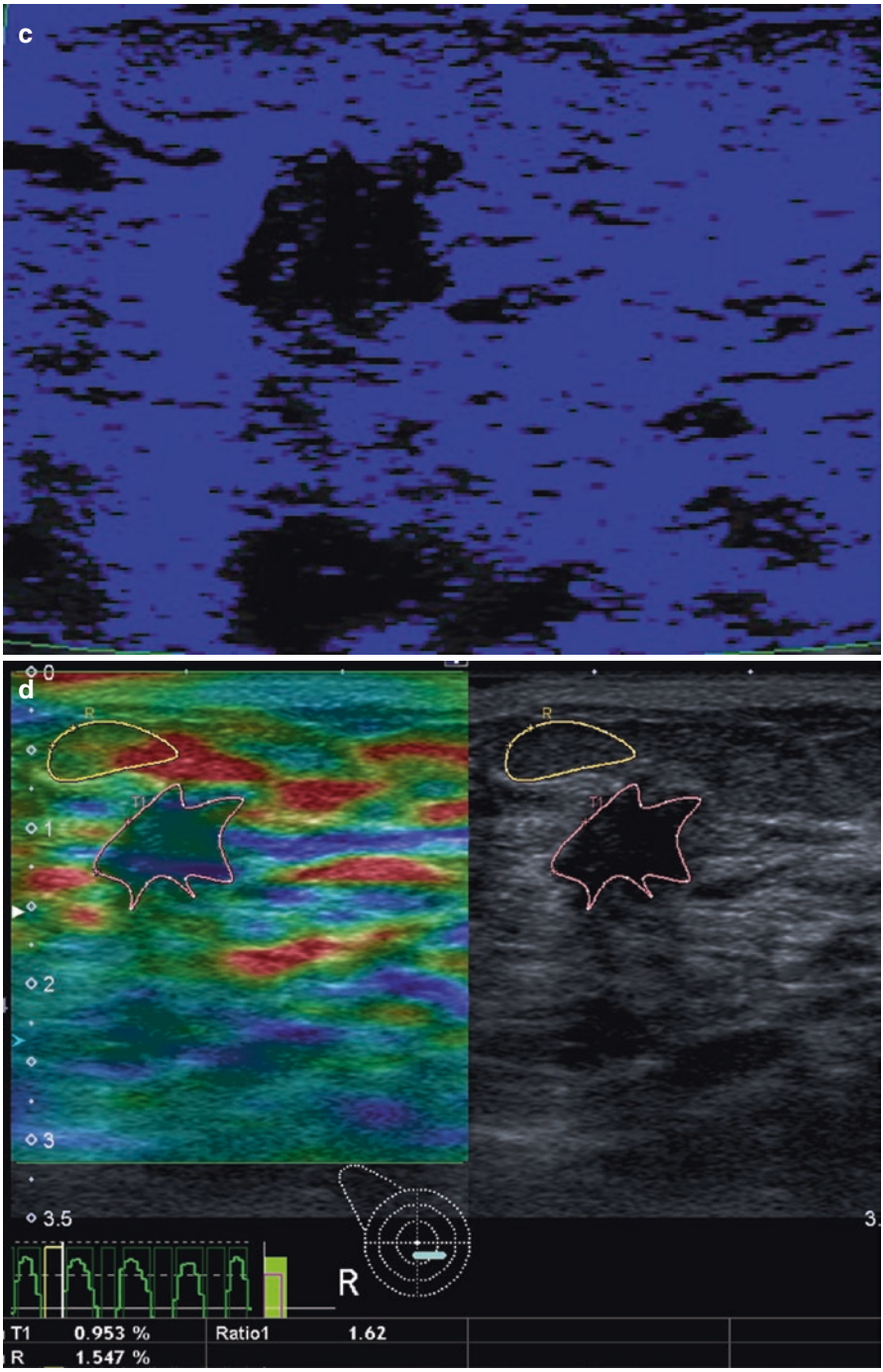

Fig. 19.1 (continued)

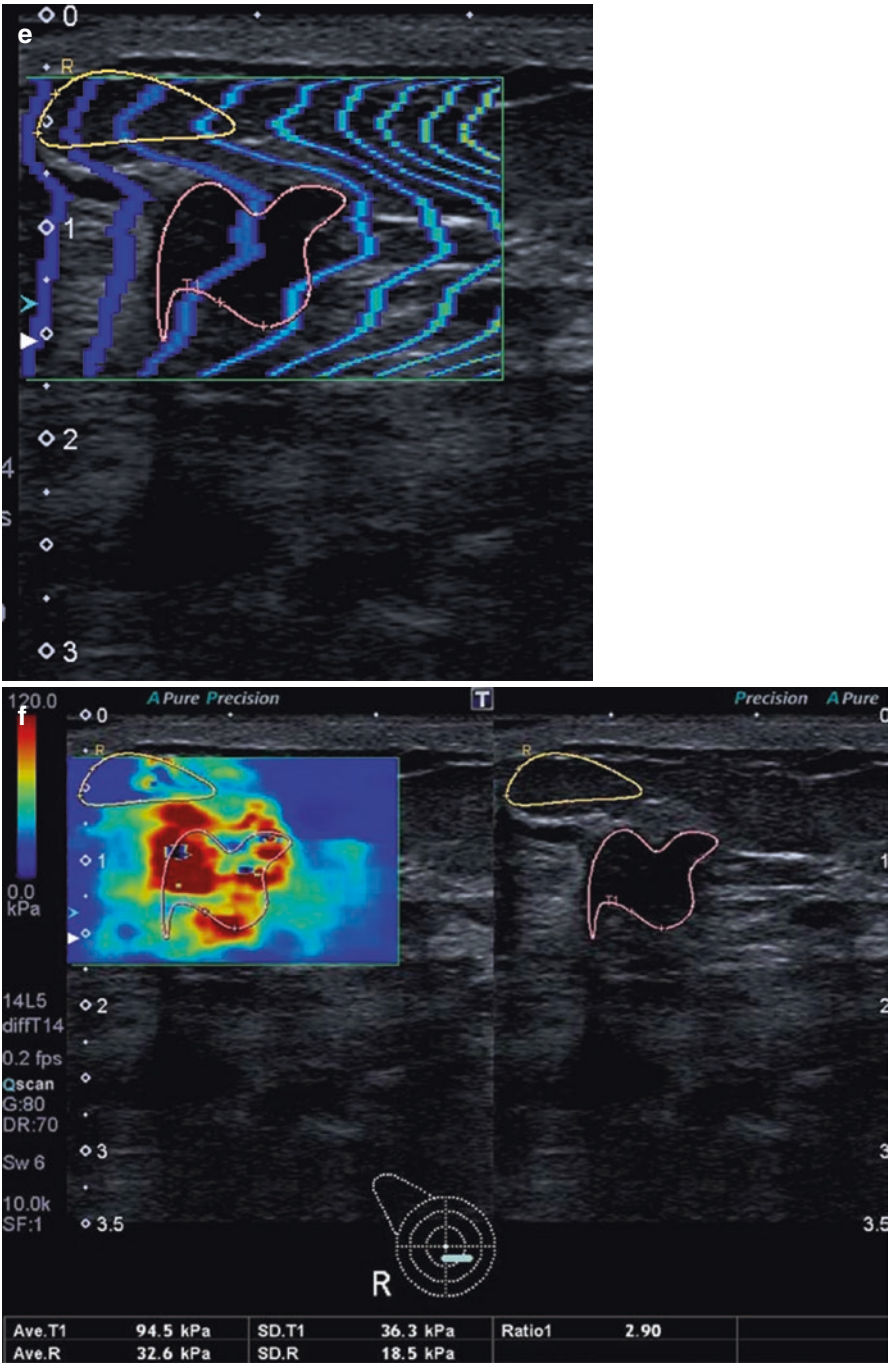

Fig. 19.1 (continued)

In real-time elastography, the examiner uses the ultrasound transducer to compress the tissue from outside the body and then to measure the resulting tissue movement or deformation. The elasticity information obtained in this way is displayed as a color map superimposed on the grayscale image in real time. In real-time elastography, many investigators use the blue color spectrum to represent low strain, which is equivalent to a high intrinsic elastic modulus (hard tissue), while green and red colors are used to indicate intermediate to high strain, i.e., low elastic modulus or soft tissue. Of note, most shear wave-based systems have a reversed scale, that is, red for stiff tissues and blue for soft (normal) tissues. State-of-the-art ultrasound systems allow free selection and reversal of the available color scales. Standardization would be desirable. In women with low breast tissue density, elastography has been found to markedly improve detection and characterization of focal lesions. In women with involuted glandular tissue, real-time elastography has been shown to increase specificity from 69 to 80%. This is important since the diagnostic accuracy of B-mode ultrasound decreases with involution of breast parenchyma. A multicenter study of 779 women has confirmed these results [14].

In the further development of sonoelastography of the breast, standardization was improved by the introduction of a *fat-to-lesion strain ratio* (*FLR*), which defines the relationship between the elasticity of fatty tissue and that of the breast lesion (Fig. 19.1d). The FLR is calculated from a region of interest (ROI) encircling the entire breast lesion and a second ROI placed in the surrounding fatty tissue and is compared individually and intraindividually [15, 19]. The most recent studies have shown that FLR calculation improves the characterization of breast lesions and allows differentiation of benign and malignant focal breast lesions. In a European patient population, an FLR cutoff value for discrimination of benign and malignant lesions ranging between 2.3 and 2.5 has been identified using different US systems, which differs from the cutoff of 3.1 defined in a population of Chinese women. These variations may be attributable to ethnic variations in normal glandular breast density, and they preclude the definition of a single standardized FLR. Nevertheless, this ratio is a simple and reproducible parameter for the characterization of known breast lesions. An FLR below the cutoff is highly indicative of a benign breast lesion, while an FLR above the cutoff is suspicious for a malignant breast tumor. A suspected malignant lesion requires confirmation by biopsy. Ultrasound elastography allows no differentiation of recurrent breast cancer from scar tissue. Scar tissue developing after surgery and radiotherapy has little intrinsic elasticity and thus has an FLR in the same range as malignant breast lesions. This is why magnetic resonance imaging (MRI) or biopsy with ultrasound guidance will continue to be necessary for ruling out cancer recurrence.

Tissue Doppler imaging (TDI) can be understood as a special pressure-independent version of strain elastography and also allows real-time analysis. Tissue reflection with TDI is very low; however, the signal has very high amplitude compared with the fast signals obtained by classic color Doppler ultrasound, where red blood cells serve as reflectors. When operated in the dual mode, information on tissue distortion is superimposed on B-mode views using red and blue as with conventional color Doppler imaging. Malignant breast lesions are characterized by the absence of color pixels, while benign lesions are filled with color pixels and typically appear markedly smaller in TDI (Fig. 19.1c). Therefore, TDI allows

significant differentiation of benign and malignant focal breast lesions ($p < 0.001$) (Fig. 19.1c). This technique is particularly easy to use and the gain in diagnostic information is immediately apparent [20]. Although it can theoretically be implemented into all ultrasound systems, TDI has not yet become established as a routine clinical procedure.

A first large meta-analysis of sonoelastography was conducted in 2012 and included 5511 breast lesions [21]. In this analysis, specificity increased from 70 to 88% with the use of elastography. The use of sonoelastography can reduce the need for breast biopsy particularly in screening populations with a low breast cancer risk. In the screening situation, however, elastography should not be used as the first ultrasound method but should ideally be used when B-mode ultrasound findings suggest a breast lesion. In contrast, when examining women with a high risk of breast cancer, the technique with the highest correct classification rate should be used. For breast examinations, this is FLR calculation, which has higher sensitivity compared with subjective assessment [22].

SWE and transient elastography (TE) rely on a different physical principle and require a special transducer. In TE, the transducer generates the classic ultrasound waves and additional low-frequency shear waves in the 50 Hz frequency range. The speed at which shear waves or transverse waves propagate in the tissue is measured to derive the tissue's elasticity modulus. This technique has gained much attention in recent years for the grading of liver fibrosis [23]. Recently, Stock et al. [24] investigated the acoustic radiation force impulse (ARFI) technique for the quantification of renal transplant fibrosis and found a correlation between elastography and histologic fibrosis grading. Only a few clinical studies have evaluated the potential of this technique for the differentiation of focal breast lesions. Two studies, Evans et al. [25] and Berg et al. [26], found SWE to increase specificity and thus improve the characterization of breast lesions (Fig. 19.1e, f). Other techniques, such as magnetic resonance elastography (MRE), hold promise for further improving imaging characterization of breast lesions. Inherent limitations of MRE such as long examination times and reduced spatial resolution can be overcome by state-of-the-art single-shot acquisition techniques and multifrequency vibration. Overall, it is expected that breast MRE will in the future be used as a short supplementary examination in patients with a clinical indication for conventional breast MRI. Another promising method for determining mechanical properties of breast tissue is tomosynthesis elastography, which uses a tomosynthesis technique to scan tissue layers before and after static distortion and image registration for the subsequent computation of distortion maps [27].

Regardless of the medical imaging modality used, elastography is a valid tool for detecting pathological differences in the cohesiveness of breast tissue. Mechanical stimulation can be used to derive diagnostic information on tissue properties otherwise requiring invasive procedures.

19.1.3 Thyroid Cancer

The anatomic location makes elastography of the thyroid more difficult than examination of the breast, where the surrounding fat can be used as reference for comparison.

Therefore, absolute elasticity properties of individual thyroid nodules need to be compared, and definition of standardized reference values is difficult. A comprehensive meta-analysis of the characterization of focal thyroid lesions by elastography is still lacking. While single-center studies suggest a benefit of elastography in characterizing thyroid nodules, elastography cannot replace cytology for a definitive diagnosis [28].

Nonpalpable thyroid nodules are a common incidental finding in asymptomatic individuals. Ultrasound is the first-line imaging modality in the workup of small incidentally detected thyroid nodules. While small nodules <1 cm in size are typically managed by follow-up, the further procedure in individuals with nodules ≥1 cm in size depends on the initial ultrasound findings and may include laboratory tests, fine-needle aspiration cytology (FNAC), and scintigraphy. Besides the general appearance at B-mode or color duplex ultrasound, a number of individual features are assessed to identify malignant thyroid nodules including echotexture/hypoechogenicity, presence of microcalcifications, absence or poorly defined margin and central hypervascularization, as well as conspicuous lymph nodes [28]. Diagnostic accuracy relies on the examiner's experience [28]. Some of the features that are typical of malignancy may also be present in benign thyroid nodules. As a result, high-resolution US has low specificity, and elastography has been investigated to determine its potential for improving the specificity of thyroid US. However, currently available data were obtained in small, selected patient populations with an indication for FNAC [29]. The first studies of thyroid sonoelastography were performed using the technique of strain elastography and manual tissue compression with the ultrasound transducer [29, 30]. Different scoring systems such as the Ueno score have been proposed (ranging from 1 for mostly soft tissue to 4/5 for completely hard tissue); however, thyroid nodule categorization using these scores has been found to have only moderate interobserver validity of <68% in unselected patient populations [29–31]. These results were improved with the introduction of semi-quantitative elasticity indices and definition of cutoff values, which resulted in reported sensitivities of 74–98% and specificities of 72–100% [32, 33]. There is agreement among investigators that strain elastography of the thyroid is a supplementary technique for improving the specificity of high-resolution B-mode ultrasound and that the sensitivity of combined B-mode ultrasound and color-coded Doppler ultrasound (CD-US) appears to be superior to elastography [32, 33].

Another approach to standardization is to exploit carotid artery pulsation for inducing pressure-dependent deformation of the thyroid, and a study has shown that this approach reduces examiner dependence [34]. Furthermore, attempts have been made, using ARFI [35] and SWE, to develop an examiner-independent technique for the measurement of the propagation velocity in m/s or of pressure in kPa. Again, cutoff values were determined to discriminate benign and malignant lesions. Initial optimistic results with specificities of 93–95% [35] were not confirmed in later studies, where specificities of 71–78% were found [1, 36]. This is below the specificity of strain elastography and suggests that examiner dependence might not be an issue. Multicenter studies should be performed in unselected patient populations with subsequent histological confirmation of findings. So far, the superior specificity of elastography mainly helps in identifying patients who should undergo FNAC. Having relatively low sensitivity, elastography cannot be recommended as

the only test for the follow-up of presumably benign thyroid nodules, and FNAC continues to be required for diagnostic confirmation.

19.1.4 Prostate Cancer

Men with an elevated prostate-specific antigen (PSA) level or abnormal prostate findings in the digital rectal examination (DRE) undergo workup by transrectal ultrasound (TRUS) in combination with systematic biopsy for histologic confirmation. In a subgroup of these patients, TRUS-guided biopsy fails to detect cancer despite increasing PSA levels, and multiple biopsies may be necessary before a diagnosis can be made [37, 38]. Since negative TRUS-guided biopsy does not rule out prostate cancer, healthy men may be repeatedly exposed to the possible risks (infection, bleeding) of this invasive procedure. Moreover, the detection rate markedly decreases with each repetition of prostate biopsy [37]. Many suggestions have been made to improve the cancer detection rate of TRUS. Since it is known that prostate cancer is associated with changes in metabolism and perfusion [39, 40], techniques such as color Doppler US and contrast-enhanced ultrasound (CEUS) at high frequency as well as elastography have been proposed for prostate cancer detection without achieving decisive progress [41]. Data on TRUS elastography are highly variable with reported sensitivities for prostate cancer detection ranging from 25 to 92% [42, 43]. A breakthrough was finally achieved by combining multiparametric 3 T MRI without the use of an endorectal coil for localizing suspicious lesions within the prostate with subsequent use of these data for real-time MRI/US fusion biopsy. Initial results with MRI/US fusion biopsy in subgroups of patients showed detection rates that were comparable to that of the time-consuming and expensive method of MRI-guided biopsy [44]. Fusion biopsy is also performed using a multiparametric approach combining color Doppler, CEUS, and elastography. The advantage of this technique is in the assessment of focal lesions in a given plane like the MRI, which also takes the high detection rate of prostate cancer by MRI into account. Both CEUS and elastography have shown high specificity in multiparametric US. Approaches for using elastography aim at identifying suspicious lesions for subsequent targeted biopsy with routine TRUS-based techniques. Of particular interest is SWE, which yields absolute values for focal lesions compared with the unaffected side. Initial publications on this technique have proposed cutoff values on the order of 35 kPa [45]. Future studies must show whether the limited penetration depth of this technique can be improved further and whether these initial results can be confirmed by multicenter trials. However, elastography has the potential to provide supplementary information that could be used for routine TRUS-guided biopsy in patients with abnormal B-mode findings.

19.1.5 Summary of Part A

Based on currently available data, routine clinical elastography could provide important additional diagnostic information for the differentiation of breast tumors,

for identifying patients with thyroid nodules (>1 cm) who should undergo FNAC, and for men with suspected prostate cancer who have abnormal B-mode ultrasound findings and are scheduled for TRUS-guided biopsy. The use of sonoelastography improves specificity and directly provides additional diagnostic information. Having high detail resolution, sonoelastography allows reliable evaluation of lesions once they have reached a size of 5 mm. Besides real-time elastography based on strain imaging, SWE will gain wider acceptance in the future as it allows quantification of parameters. With ultrasound having a minor role in the classification of tumors, as discussed here for different cancers, the expected role of elastography is also limited; however, this should not prevent researchers from considering all tumors of a specialty when evaluating the potential of a new imaging modality. In addition, larger studies should investigate whether elastography yields adequate results for various diagnostic queries even in the hands of less experienced examiners. Papillary thyroid cancer appears to be harder than follicular and medullary thyroid cancer. Invasive ductal carcinoma is harder than invasive lobular breast tumors. This is where elastography has the potential for identifying tumor subgroups. Nevertheless, sound statistical data or evidence from large multicenter studies is still lacking. Not all malignant tumors are hard and not all benign tumors are soft, which is a fundamental limitation of elastography. On the other hand, sonoelastography requires little extra time and the cost is very low. These advantages make sonoelastography an attractive option and could contribute to its wider use in different diagnostic settings.

19.2 Part B: Contrast-Enhanced Ultrasound

19.2.1 Introduction

The visualization of tissue properties and tissue perfusion is an important component of the diagnostic evaluation of tumors and kidneys and in trauma patients by any imaging modality. Conventional vascular ultrasound (US) techniques such as color duplex ultrasonography (CDUS) do not depict vessels with a diameter of less than about 30 mm. Furthermore, this method is susceptible to error due to examiner dependence and the effect of systemic disease such as atherosclerosis which often results in artifacts and posterior acoustic shadowing. The advent of nonspecific ultrasound contrast media (USCM) has markedly improved the detection of very slow blood flow in small vessels. The potential of target-specific USCM for demonstrating neoangiogenesis in cancer is a new approach. Possible candidates for such a contrast agent are microbubbles to which a vascular endothelial growth factor receptor 2 (VEGFR2)-binding peptide or antigen is coupled, which selectively mark areas of tumor neoangiogenesis. Unspecific USCM might be superior in the diagnosis of abnormal tumor perfusion compared with conventional US since tumor perfusion is associated with characteristic changes of the arterial inflow and the late washout phase of the contrast agent.

19.2.2 Contrast-Enhanced Ultrasound of the Liver

In 2001, phospholipid-stabilized microbubbles of a poorly water-soluble gas (e.g., sulfur hexafluoride, SF6, SonoVue®) became commercially available as a second-generation ultrasound contrast agent [46]. This microbubble preparation is very stable, providing prolonged contrast and enhancing the ultrasound signal in blood vessels including the capillary system by several orders of magnitude (by a factor of approx. 103). The SonoVue microbubbles have a mean diameter of 2.5 μm and are smaller than red blood cells (7 μm), allowing them to distribute freely in the blood vessels and capillaries [47–50].

When exposed to low ultrasound energy, the microbubbles generate only linear backscatter. With increasing energy, once certain range is reached, the microbubbles begin to oscillate at eigenfrequency with a characteristic resonance spectrum. Following injection into a peripheral vein, the microbubbles will reach the organs and distribute in their capillary beds, resulting in homogeneous opacification of normally perfused organs or parts [51]. State-of-the-art ultrasound devices can be operated in a special mode to sample and process the specific nonlinear reflection from the microbubbles for selective visualization with very high temporal resolution of parenchymal perfusion (typically as color-coded information) [47].

Unlike conventional CT and MRI contrast agents, the ultrasound microbubbles do not diffuse into the interstitial space, and they are not eliminated by the kidneys but are exhaled via the lungs within a few minutes [48, 52]. Ultrasound contrast agents are considered to be very safe because they are biologically inert, are not nephrotoxic, and do not interact with the thyroid, and the incidence of allergic reactions following microbubble administration is well below that of conventional CT contrast agents [53].

One of the strengths of CEUS is the high temporal resolution of perfusion visualization compared with other imaging modalities. The safety profile of ultrasound contrast agents allows repeated administration in serial follow-up examinations at short intervals [52].

Ultrasound is usually the first-line imaging modalities for diagnostic evaluation of patients with metastatic liver lesions. Focal liver lesions are common, with a reported prevalence of approx. 5% [54]. Liver ultrasound is performed at a frequency range of 2–9 MHz (Figs. 19.2 and 19.3).

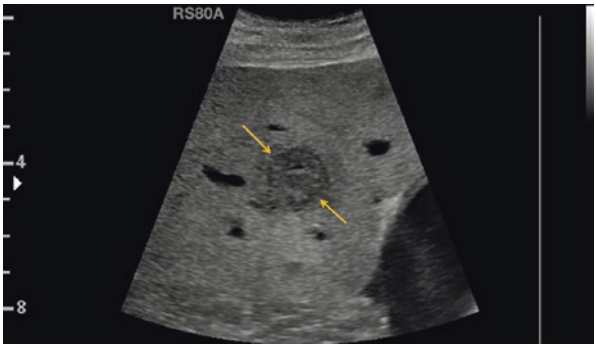

Fig. 19.2 In this patient with suspected pharyngeal cancer, abdominal staging by standard B-mode ultrasound reveals a hypoechoic liver lesion (*yellow arrows*)

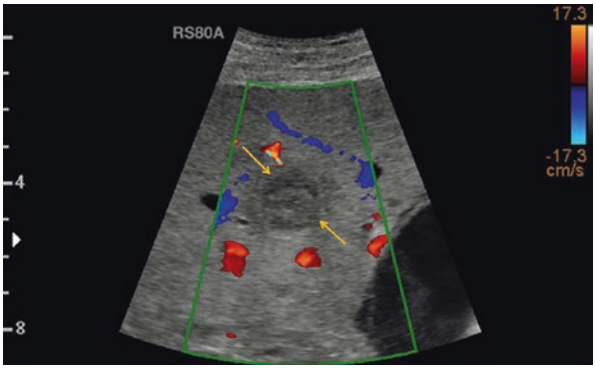

Fig. 19.3 The lesion (*yellow arrows*) does not have increased vascularization on color flow imaging (see patient description in Fig. 19.2)

The liver is the main target of metastatic disease with 25–50% of all cancer patients having liver metastases at the time of diagnosis [55]. The treatment options (surgical resection versus interventional treatment) depend on the size, number, and localization of liver metastases [56, 57]. This is why reliable detection and characterization of liver lesions is crucial for estimating the prognosis and the choice of treatment [58, 59]. In a meta-analysis, Kinkel et al. found the detection rate for liver metastases of gastrointestinal malignancies to be only 55% for B-mode ultrasound versus 72%, 76%, and 90% for contrast-enhanced CT, MRI, and PET, respectively [60, 61].

The advent of CEUS in 2001 fundamentally changed the diagnostic accuracy of ultrasound. In a German multicenter study, CEUS correctly characterized approx. 90% of focal liver lesions [58].

The EFSUMB Guidelines distinguish three phases of contrast enhancement in ultrasound: an arterial phase lasting until approx. 30 s after injection, a portal venous phase from 30 to 120 s, and a late phase after 120 s [62–64].

Benign liver lesions such as focal nodular hyperplasia (FNH) and hemangioma are characterized by isoenhancement to hyperenhancement in the late phase. The most important criterion distinguishing malignant from benign liver lesions is washout of the contrast agent in the late phase. Depending on the primary cancer, washout of a liver metastasis may begin in the late arterial phase and is nearly always seen in the portal venous phase (Figs. 19.4, 19.5, and 19.6).

In addition, CEUS can improve the monitoring of interventional treatment such as radiofrequency ablation (RFA) or transarterial chemoembolization (TACE) and intraoperative interventions [65, 66].

19.2.3 Summary of Part B

Ultrasound is usually the first-line imaging modalities for diagnostic evaluation of patients with metastatic liver lesions. The advent of CEUS fundamentally changed the diagnostic accuracy of ultrasound. CEUS can improve the monitoring of

Fig. 19.4 Following administration of the ultrasound contrast agent, there is strong marginal enhancement of the lesion in the arterial phase (*white arrows*, see patient description in Fig. 19.2)

Fig. 19.5 In the portal venous phase, the lesion (*white arrows*) is demarcated from surrounding liver parenchyma by beginning washout (see patient description in Fig. 19.2)

Fig. 19.6 In the late phase, there is increasing washout of the lesion (*white arrows*), confirming the diagnosis of a liver metastasis based in morphologic imaging. The subsequent liver biopsy confirmed liver metastasis from a poorly differentiated nonkeratinizing squamous cell carcinoma (see patient description in Fig. 19.2)

interventional treatment and the follow-up of tumor patients under drug treatment and monitor the effect of interventions. Ultrasound contrast agents are considered to be very safe because they are biologically inert, are not nephrotoxic, and do not interact with the thyroid, and the incidence of allergic reactions following microbubble administration is well below that of conventional CT contrast agents.

Conclusion

Meanwhile elastography and perfusion measurements have been established as clinical routine methods of ultrasound examinations. Quantifications of elasticity and perfusion provide objective parameters for tumor stiffness and specific perfusion. Ultrasound contrast agents and elastography are considered to be very safe because they are biologically inert. Many cancer entities show characteristic differences in terms of elastographic properties compared with surrounding tissue. Here, elastography can improve targeted biopsy for the workup of suspicious focal lesions. Elastography has been demonstrated to be superior to routine biopsy guided by B-mode ultrasound. CEUS has high diagnostic accuracy and is comparable to CT and MRI in terms of tumor characterization. Having a low rate of adverse effects, CEUS can be used in patients with impaired renal function or contraindications to CT or MRI contrast agents. Quantifiable elastography and CEUS have recently started to expand the role of classic B-mode ultrasound in oncology. Quantification of tumor stiffness and perfusion can improve the differential diagnosis. These two ultrasound techniques are beginning to enter the clinic and offer a fascinating potential for further advances including improved standardization of ultrasound diagnosis.

References

1. Céspedes I, Ophir J, Ponnekanti H, et al. Elastography: elasticity imaging using ultrasound with application to muscle and breast in vivo. Ultrason Imaging. 1993;15:73–88.
2. Garra BS, Cespedes EI, Ophir J, et al. Elastography of breast lesions: Initial clinical results. Radiology. 1997;202:79–86.
3. Krouskop TA, Wheeler TM, Kallel F, et al. Elastic moduli of breast and prostate tissues under compression. Ultrason Imaging. 1998;20:260–74.
4. Konofagou E, Ophir J. A new elastographic method for estimation and imaging of lateral displacements, lateral strains, corrected axial strains and Poisson's ratios in tissues. Ultrasound Med Biol. 1998;24:1183–99.
5. Frey H. Realtime-elastographie. Ein neues sonographisches verfahren für die darstellung der gewebeelastizität. Radiologe. 2003;43(10):850.
6. Klintworth N, Mantsopoulos K, Zenk J, et al. Sonoelastography of parotis gland tumours: initial experience and identification of characteristics patterns. Eur Radiol. 2012;22:947–56. https://doi.org/10.1007/s00330-011-2344-7.
7. Rubaltelli L, Corradin S, Dorigo A, et al. Differential diagnosis of benign and malignant thyroid nodules at elastosonography. Ultraschall Med. 2009;30:175–9. https://doi.org/10.1055/s-2008-1027442.
8. Hong Y, Liu X, Li Z, et al. Real-time ultrasound elastography in the differential diagnosis in benign and malignant thyroid nodules. J Ultrasound Med. 2009;28:861–7.
9. Kanamoto M, Shimada M, Ikegami T, et al. Real time elastography for noninvasive diagnosis in liver fibrosis. J Hepato-Biliary-Pancreat Surg. 2009;16:463–7. https://doi.org/10.1007/s00534-009-0075-9.
10. Friedrich-Rust M, Nierhoff J, Lupsor M, et al. Performance of acoustic radiation force impulse imaging for the staging of liver fibrosis: a pooled meta-analysis. J Viral Hepat. 2012;19:e212–9. https://doi.org/10.1111/j.1365-2893.2011.01537.x.
11. Aigner F, Pallwein L, Junker D, et al. Value of real-time elastography targeted biopsy for prostate cancer detection in men with prostate specific antigen 1.25 ng/ml or greater and 4.00 ng/ml or less. J Urol. 2010;184:913–7. https://doi.org/10.1016/j.juro.2010.05.026.

12. Thomas A, Kümmel S, Gemeinhardt O, et al. Real-time sonoelastography of the cervix: tissue elasticity of the normal and abnormal cervix. Acad Radiol. 2007;14:193–200.
13. Thomas A, Kümmel S, Fritzsche F, et al. Real-time sonoelastography performed in addition to B-mode ultrasound and mammography: improved differentiation of breast lesions? Acad Radiol. 2006;13:1496–504.
14. Wojcinski S, Farrokh A, Weber S, et al. Multicenter study of ultrasound real-time tissue elastography in 779 cases for the assessment of breast lesions: improved diagnostic performance by combining the BI-RADS®-US classification system with sonoelastography. Ultraschall Med. 2010;31:484–91. https://doi.org/10.1055/s-0029-1245282.
15. Thomas A, Degenhardt F, Farrokh A, et al. Significant differentiation of focal breast lesions: calculation of strain ratio in breast sonoelastography. Acad Radiol. 2010;17:558–63. https://doi.org/10.1016/j.acra.2009.12.006.
16. Itoh A, Ueno E, Tohno E, et al. Breast disease: clinical application of US elastography for diagnosis. Radiology. 2006;239:341–50.
17. Thomas A, Fischer T, Ohlinger R, et al. An advanced method of ultrasound - real-time elastography: first experience on 106 patients with breast lesions. Ultrasound Obstet Gynecol. 2006;28:335–40.
18. D'Orsi CJ, Sickles EA, Mendelson EB, et al. ACR BI-RADS® atlas, breast imaging reporting and data system. Reston: American College of Radiology; 2013.
19. Fischer T, Peisker U, Fiedor S, et al. Significant differentiation of focal breast lesions: raw data-based calculation of strain ratio. Ultraschall Med. 2012;33:372–9.
20. Thomas A, Warm M, Diekmann F, et al. Tissue doppler and strain imaging for evaluating tissue elasticity of breast lesions. Acad Radiol. 2007;14:522–9.
21. Sadigh G, Carlos RC, Neal CH, et al. Ultrasonographic differentiation of malignant from benign breast lesions: a meta-analytic comparison of elasticity and BIRADS scoring. Breast Cancer Res Treat. 2012;133:23–35. https://doi.org/10.1007/s10549-011-1857-8.
22. Sadigh G, Carlos RC, Neal CH, et al. Accuracy of quantitative ultrasound elastography for differentiation of malignant and benign breast abnormalities: a meta-analysis. Breast Cancer Res Treat. 2012;134:923–31. https://doi.org/10.1007/s10549-012-2020-x.
23. Friedrich-Rust M, Schwarz A, Ong M, et al. Real-time tissue elastography versus FibroScan for noninvasive assessment of liver fibrosis in chronic liver disease. Ultraschall Med. 2009;30:478–84. https://doi.org/10.1055/s-0028-1109488.
24. Stock KF, Klein BS, Vo Cong MT, et al. ARFI-based tissue elasticity quantification in comparison to histology for the diagnosis of renal transplant fibrosis. Clin Hemorheol Microcirc. 2010;46:139–48. https://doi.org/10.3233/CH-2010-1340.
25. Evans A, Whelehan P, Thomson K, et al. Differentiating benign from malignant solid breast masses: value of shear wave elastography according to lesion stiffness combined with greyscale ultrasound according to BI-RADS classification. Br J Cancer. 2012;107:224–9. https://doi.org/10.1038/bjc.2012.253.
26. Berg WA, Cosgrove DO, Doré CJ, et al. Shear-wave elastography improves the specificity of breast US: the BE1 multinational study of 939 masses. Radiology. 2012;262:435–49. https://doi.org/10.1148/radiol.11110640.
27. Engelken FJ, Sack I, Klatt D, et al. Evaluation of tomosynthesis elastography in a breast-mimicking phantom. Eur J Radiol. 2012;81:2169–73. https://doi.org/10.1016/j.ejrad.2011.06.033.
28. Carneiro-Pla D. Ultrasound elastography in the evaluation of thyroid nodules for thyroid cancer. Curr Opin Oncol. 2013;25:1–5. https://doi.org/10.1097/CCO.0b013e32835a87c8.
29. Bhatia KS, Rasalkar DP, Lee YP, et al. Cystic change in thyroid nodules: a confounding factor for real-time qualitative thyroid ultrasound elastography. Clin Radiol. 2011;66:799–807. https://doi.org/10.1016/j.crad.2011.03.011.
30. Shuzhen C. Comparison analysis between conventional ultrasonography and ultrasound elastography of thyroid nodules. Eur J Radiol. 2012;81:1806–11. https://doi.org/10.1016/j.ejrad.2011.02.070.
31. Kim JK, Baek JH, Lee JH, et al. Ultrasound elastography for thyroid nodules: a reliable study? Ultrasound Med Biol. 2012;38:1508–13. https://doi.org/10.1016/j.ultrasmedbio.2012.05.017.

32. Xing P, Wu L, Zhang C, et al. Differentiation of benign from malignant thyroid lesions: calculation of the strain ratio on thyroid sonoelastography. J Ultrasound Med. 2011;30:663–9.
33. Ragazzoni F, Deandrea M, Mormile A, et al. High diagnostic accuracy and interobserver reliability of real-time elastography in the evaluation of thyroid nodules. Ultrasound Med Biol. 2012;38:1154–62. https://doi.org/10.1016/j.ultrasmedbio.2012.02.025.
34. Lim DJ, Luo S, Kim MH, et al. Interobserver agreement and intraobserver reproducibility in thyroid ultrasound elastography. Am J Roentgenol. 2012;198:896–901. https://doi.org/10.2214/AJR.11.7009.
35. Friedrich-Rust M, Romenski O, Meyer G, et al. Acoustic radiation force impulse-imaging for the evaluation of the thyroid gland: a limited patient feasibility study. Ultrasonics. 2012;52:69–74. https://doi.org/10.1016/j.ultras.2011.06.012.
36. Sebag F, Vaillant-Lombard J, Berbis J, et al. Shear wave elastography: a new ultrasound imaging mode for the differential diagnosis of benign and malignant thyroid nodules. J Clin Endocrinol Metab. 2010;95:5281–8. https://doi.org/10.1210/jc.2010-0766.
37. Djavan B, Ravery V, Zlotta A, et al. Prospective evaluation of prostate cancer detected on biopsies 1, 2, 3 and 4: when should we stop? J Urol. 2001;166:1679–83.
38. Presti JC Jr. Repeat prostate biopsy–when, where, and how. Urol Oncol. 2009;27:312–4. https://doi.org/10.1016/j.urolonc.2008.10.029.
39. Frauscher F, Pallwein L, Klauser A, et al. Ultrasound contrast agents and prostate cancer. Radiologe. 2005;45:544–51.
40. Fischer T, Paschen CF, Slowinski T, et al. Differentiation of parotid gland tumors with contrast-enhanced ultrasound. RöFo. 2010;182:155–62. https://doi.org/10.1055/s-0028-1109788.
41. Pallwein L, Mitterberger M, Gradl J, et al. Value of contrast-enhanced ultrasound and elastography in imaging of prostate cancer. Curr Opin Urol. 2007;17:39–47.
42. Yan Z, Jie T, Yan-Mi L, et al. Role of transrectal real-time tissue elastography in the diagnosis of prostate cancer. Zhongguo Yi Xue Ke Xue Yuan Xue Bao. 2011;33:175–9. https://doi.org/10.3881/j.issn.1000-503X.2011.02.015.
43. Nelson ED, Slotoroff CB, Gomella LG, et al. Targeted biopsy of the prostate: the impact of color Doppler imaging and elastography on prostate cancer detection and Gleason score. Urology. 2007;70:1136–40.
44. Maxeiner A, Stephan C, Durmus T, et al. Added value of multiparametric ultrasonography in magnetic resonance imaging and ultrasonography fusion-guided biopsy of the prostate in patients with suspicion for prostate cancer. Urology. 2015;86(1):108–14. https://doi.org/10.1016/j.urology.2015.01.055.
45. Correas JM, Tissier AM, Khairoune A, et al. Prostate cancer: diagnostic performance of real-time shear-wave elastography. Radiology. 2015;275(1):280–9. https://doi.org/10.1148/radiol.14140567.
46. Schneider M. SonoVue, a new ultrasound contrast agent. Eur Radiol. 1999;9:S347–8.
47. Greis C. Ultrasound contrast agents as markers of vascularity and microcirculation. Clin Hemorheol Microcirc. 2009;43(1):1–9. https://doi.org/10.3233/CH-2009-1216.
48. Clevert DA, Jung EM. Interventional sonography of the liver and kidneys. Radiologe. 2013;53:962–73. https://doi.org/10.1007/s00117-012-2459-0.
49. Jung EM, Clevert DA. Possibilities of sonographic image fusion: current developments. Radiologe. 2015;55:937–48. https://doi.org/10.1007/s00117-015-0025-2.
50. Schwarz F, Sommer WH, Reiser M, et al. Contrast enhanced sonography for blunt force abdominal trauma. Radiologe. 2011;51:475–82. https://doi.org/10.1007/s00117-010-2103-9.
51. Valentino M, Serra C, Pavlica P, et al. Contrast-enhanced ultrasound for blunt abdominal trauma. Semin Ultrasound CT MR. 2007;28:130–40.
52. Claudon M, Cosgrove D, Albrecht T, et al. Guidelines and good clinical practice recommendations for contrast enhanced ultrasound (CEUS) - update 2008. Ultraschall Med. 2008;29:28–44. https://doi.org/10.1055/s-2007-963785.
53. Piscaglia F, Bolondi L, Italian Society for Ultrasound in Medicine and Biology (SIUMB) Study Group on Ultrasound Contrast Agents. The safety of Sonovue® in abdominal applications: retrospective analysis of 23188 investigations. Ultrasound Med Biol. 2006;32(9):1369–75.

54. Strobel DB. Diagnostik bei fokalen Leberläsionen. Dtsch Arztebl Int. 2006;103:789–93.
55. Oldenburg A, Hohmann J, Foert E, et al. Detection of hepatic metastases with low MI real time contrast enhanced sonography and SonoVue. Ultraschall Med. 2005;26:277–84.
56. Harvey CJ, Blomley MJ, Eckersley RJ, et al. Developments in ultrasound contrast media. Eur Radiol. 2001;11:675–89.
57. Clevert DA, D'Anastasi M, Jung EM. Contrast-enhanced ultrasound and microcirculation: efficiency through dynamics–current developments. Clin Hemorheol Microcirc. 2013;53(1-2):171–86. https://doi.org/10.3233/CH-2012-1584.
58. Regge D, Campanella D, Anselmetti GC, et al. Diagnostic accuracy of portal-phase CT and MRI with mangafodipir trisodium in detecting liver metastases from colorectal carcinoma. Clin Radiol. 2006;61(4):338–47.
59. Jung EM, Wiggermann P, Stroszczynski C, et al. Ultrasound diagnostics of diffuse liver diseases. Radiologe. 2012;52(8):706–16. https://doi.org/10.1007/s00117-012-2307-2.
60. Kinkel K, Lu Y, Both M, et al. Detection of hepatic metastases from cancers of the gastrointestinal tract by using noninvasive imaging methods (US, CT, MR imaging, PET): a meta-analysis. Radiology. 2002;224(3):748–56.
61. Weskott HP. Detection and characterization of liver metastases. Radiologe. 2011;51:469–74. https://doi.org/10.1007/s00117-010-2100-z.
62. Strobel D, Seitz K, Blank W, et al. Contrast-enhanced ultrasound for the characterization of focal liver lesions – diagnostic accuracy in clinical practice1 (DEGUM multicenter trial). Ultraschall Med. 2008;29:499–505. https://doi.org/10.1055/s-2008-1027806.
63. Claudon M, Dietrich CF, Choi BI, et al. Guidelines and good clinical practice recommendations for contrast enhanced ultrasound (CEUS) in the liver–update 2012: a WFUMB-EFSUMB initiative in cooperation with representatives of AFSUMB, AIUM, ASUM, FLAUS and ICUS. Ultraschall Med. 2013;34:11–29. https://doi.org/10.1055/s-0032-1325499.
64. Clevert DA, Helck A, Paprottka PM, et al. Latest developments in ultrasound of the liver. Radiologe. 2011;51:661–70. https://doi.org/10.1007/s00117-010-2124-4.
65. Clevert DA, Paprottka PM, Helck A, et al. Image fusion in the management of thermal tumor ablation of the liver. Clin Hemorheol Microcirc. 2012;52:205–16. https://doi.org/10.3233/CH-2012-1598.
66. Clevert DA, Helck A, Paprottka PM, et al. Ultrasound-guided image fusion with computed tomography and magnetic resonance imaging. Clinical utility for imaging and interventional diagnostics of hepatic lesions. Radiologe. 2012;52:63–9. https://doi.org/10.1007/s00117-011-2252-5.